Geomechanics and Engineering, *Vol. 46, No. 1 (2026) 53-69*
https://doi.org/10.12989/gae.2026.46.1.053

Techno-Press

Statistical evaluation of lateral interpretation criteria for flexible pre-bored PC piles in drained soils

Xing-Ji Wang[1], Yit-Jin Chen*[1], Mary Abigail Jos[1], Anjerick Topacio[2]

[1]*Department of Civil Engineering, Chung Yuan Christian University, Chung-Li, Taiwan*
[2]*Department of Civil, Industrial, and Mechanical Engineering, Lyceum of the Philippines University – Cavite, Cavite, Philippines*

(Received January 9, 2026, Revised April 30, 2026, Accepted May 7, 2026)

Abstract. This study evaluates the lateral capacity of flexible pre-bored precast concrete (PC) piles under drained soil conditions by employing various representative interpretation criteria. A database comprising 15 field lateral load tests in Taiwan was analyzed to investigate the relationships and reliability among various displacement, rotation, and graphical-based interpretation methods. Results show that the mean interpreted Q/Q_H ratios for displacement and rotation-based methods range from 0.20 to 0.80, increasing with larger movements. For graphical methods, the ratios are $Q_{S\&W}/Q_H$ = 0.42 and Q_L/Q_H = 0.59, with standard deviations and coefficients of variation comparable to other criteria. The Q_L method provided the most reasonable and consistent evaluation of both capacity and displacement, corresponding closely to the load at 20 mm or 3% of the pile diameter. Regression analysis identified $Q_{10\%B}$ as the most reliable predictor, with a high coefficient of determination (r^2 = 0.92). Overall, pre-bored PC piles exhibited higher normalized lateral capacities than drilled shafts and driven piles. The findings provide practical guidance for the consistent interpretation and design of flexible pre-bored PC piles under lateral loading.

Keywords: database; interpretation criteria; lateral capacity; load tests; pre-bored PC piles

1. Introduction

While axial capacity has long been the primary focus of analysis and design of pile foundations, lateral capacity is equally important, particularly for structures subjected to significant horizontal loads such as earthquakes and wind [1, 2]. Ensuring the reliability of lateral capacity is essential not only for stability but also for serviceability, because excessive lateral displacements and rotations can compromise structural performance and functionality.

The ultimate lateral capacity of pile foundations generally occurs at relatively large displacements or rotations. In practical design, however, allowable displacements and rotations must be limited to meet serviceability requirements. As a result, the “lateral design capacity” of pile foundations, including pre-bored precast concrete (PC) piles, is usually inferred from lateral load test results, often called as the “interpreted failure load”.

The lateral capacity and behavior of piles have been widely studied and evaluated in both research and practice [1-8]. There have been studies on the lateral loads for flexible piles [9, 10].

*Corresponding author, Ph.D., E-mail: yjc@cycu.edu.tw

http://www.techno-press.org/gae/5

ISSN: 2005-307X (Print), 2092-6219 (Online)

Over the years, various interpretation criteria have been proposed to define lateral capacity based on load test results. These methods are founded on different assumptions: some depend on subjective judgment and the scale of the test curve, while others involve extrapolation of measured data. As a result, the interpreted capacities often differ considerably. Such methods have been evaluated extensively for drilled shafts, but the case of pre-bored PC piles has received less attention.

Pre-bored PC piles differ in construction from conventional drilled piles such as drilled shafts, and this distinction influences their load-transfer mechanisms. The construction process typically involves pre-boring, placing cement grout, and lowering the PC pile into position [11]. The presence of the cement grout affects both axial and lateral responses, leading to potential differences in capacity mobilization compared with traditional deep foundations. While recent studies evaluated the axial compression and uplift capacity of pre-bored PC piles [11-13], a comprehensive evaluation of their lateral performance remains lacking. Most existing lateral interpretation criteria rely on data from drilled shafts, which may not accurately reflect the behavior of the pre-bored PC piles. Given the increasing application of these piles in urban and infrastructure projects, establishing reliable and consistent lateral interpretation criteria is of significant engineering importance.

The objective of this paper is to evaluate and compare representative interpretation criteria for determining the lateral capacity of flexible pre-bored PC piles under drained soils. A database of lateral load tests is analyzed to examine the relative merits, interrelationships, and reliability of different criteria. The interpreted capacities are then compared both statistically and graphically. Additionally, the data in this study will be integrated into a broader pile load test database [14-16]. These high-quality datasets are essential for the advancement of data-centric geotechnics, which is a data-driven approach in geotechnical engineering that utilizes real-world data to support digital transformation and decision making, specifically for training artificial intelligence models to improve the accuracy of future capacity predictions [13, 17, 18]. From the results, recommendations are made for the consistent application of interpretation criteria in practice.

2. Database of lateral load tests

The database developed for this study consists of 15 field lateral load tests conducted on pre-bored PC piles in Taiwan under drained soil conditions. The basic soil and pile information is summarized in Table 1, while the material parameters are presented in Table 2. Fig. 1 shows the horizontal load versus pile displacement for each lateral load test. To account for the behavior of the interface formed by cement grout between the pile and the surrounding soil, the concrete strength of the pile and the strength of the cement grout were combined to simulate the actual conditions at the failure interface. The commonly adopted compressive strengths of concrete (f'_c) for pre-bored PC piles are 49.03 MPa (500 kg/cm^2) and 78.45 MPa (800 kg/cm^2). When the compressive strength is not specified in the test report, a value of 49.03 MPa (500 kg/cm^2) is assumed. The cement grout strength (f'_s) at the second interface is taken as 20.59 MPa (210 kg/cm^2), and the thickness of the cement grout is assumed to be 0.05 m.

References for the pile load tests are listed in Table 3. The pile lengths range from 20 m to 40 m, with diameters between 0.5 m and 0.8 m. The soil conditions are characterized by SPT-N values from 9 to 17 blows, soil unit weights between 16.8 and 19.4 kN/m^3, and effective friction angles ranging from 29° to 32°. The initial modulus of subgrade reaction varies from 12.11 to

Table 1. Soil and pile properties of load test data for pre-bored PC piles in drained soils

Pile No.	Test site	Soil profile	Pile Length L (m)	Pile Dia. B (m)	GWT (m)	D_r (%)	SPT-N	γ_t (kN/m^3)	φ' (°)	K_h (MN/m^3)	E_s (MPa)
PDL1	Yilan, Yilan, Taiwan	Clayey and sandy silt	40	0.6	1.0	30	9	18.0	29.3	12.11	3.92
PDL2	Fangyuan, Changhua, Taiwan	Silty sand with silt and sand	30	0.6	1.0	44	16	19.4	31.5	19.86	5.80
PDL3	Xianxi, Changhua, Taiwan	Sandy silt and silty sand	28	0.6	1.0	27	9	16.8	29.0	13.09	3.30
PDL4	Mailiao, Yunlin, Taiwan	Silty sand	25	0.5	1.5	41	13	17.9	30.8	18.72	5.08
PDL5	Mailiao, Yunlin, Taiwan	Silty sand	24	0.6	1.5	41	13	17.9	30.8	18.72	5.08
PDL6-1	Mailiao, Yunlin, Taiwan	Silty sand	25	0.5	1.9	41	13	17.9	30.8	18.72	5.08
PDL6-2	Mailiao, Yunlin, Taiwan	Silty sand	25	0.5	1.9	41	13	17.9	30.8	18.72	5.08
PDL7	Xingang, Chiayi, Taiwan	Sandy silt and silty sand	25	0.5	-	43	15	19.9	31.4	19.88	5.51
PDL8	Anping, Tainan, Taiwan	Silty sand	26	0.5	2.3	46	17	18.7	32.4	21.66	5.66
PDL9	Rende, Tainan, Taiwan	Sandy silt, clay	24	0.5	2.7	41	14	17.5	31.2	18.57	4.55
PDL10-1	Xinshi, Tainan, Taiwan	Silty sand with clay	29	0.8	1.8	43	15	19.2	31.9	20.27	5.87
PDL10-2	Xinshi, Tainan, Taiwan	Silty sand with clay	29	0.6	1.8	43	15	19.2	31.9	20.27	5.87
PDL10-3	Xinshi, Tainan, Taiwan	Silty sand with clay	29	0.8	1.8	43	15	19.2	31.9	20.27	5.87
PDL10-4	Xinshi, Tainan, Taiwan	Silty sand with clay	29	0.6	1.8	43	15	19.2	31.9	20.27	5.87
PDL11	Fengshan, Kaohsiung, Taiwan	Silty sand with clay	20.6	0.7	2.5	42	15	18.4	31.3	19.26	6.74
		n	15	15	14	15	15	15	15	15	15
		Mean	27.2	0.6	1.8	40.6	13.8	18.5	31.1	18.7	5.29
		SD	4.24	0.01	0.51	4.96	2.2	0.83	0.91	2.54	0.83
		COV	0.16	0.17	0.29	0.12	0.16	0.04	0.03	0.14	0.16

Notes: GWT = ground water table; D_r = relative density; γ_t = total unit weight; φ' = effective friction angle; K_h = initial modulus of subgrade reaction [21]; E_s = elastic modulus for soil [22]

21.66 MN/m², while the soil elastic modulus ranges from 3.92 to 6.74 MPa.

All tests were performed on flexible pre-bored PC piles, with flexibility classified according to the criteria of Broms [3] and Poulos and Hull [19]. According to Broms [3], a pile is considered flexible if it satisfies the condition $\beta_r L > 2.5$, where

$$\beta_r = \left(\frac{K_h L}{4E_c I_c}\right)^{\frac{1}{4}} \tag{1}$$

Here, β_r is the stiffness ratio between the soil and the pile, K_h is the coefficient of horizontal subgrade reaction, L is the pile length, E_c is the elastic modulus of concrete, and I_c is the moment of inertia of the pile cross-section. According to Poulos and Hull [19], a pile is flexible if its length L exceeds the critical pile length L_c, defined as

$$L_c = 4.44\left(\frac{E_c I_c}{E_s}\right)^{\frac{1}{4}} \tag{2}$$

Table 2. Material parameters for pre-bored PC piles in drained soils

Pile No.	E_c (MPa)	f'_c (MPa)	I_c (m^4)	β_r (1/cm)	$\beta_r L$
PDL1	114855	58.63	0.00636	0.00224	8.94
PDL2	94023	39.29	0.00636	0.00266	7.97
PDL3	94023	39.29	0.00636	0.00240	6.71
PDL4	93783	39.09	0.00307	0.00300	7.51
PDL5	94023	39.29	0.00636	0.00262	6.28
PDL6-1	93783	39.09	0.00307	0.00300	7.51
PDL6-2	93783	39.09	0.00307	0.00300	7.51
PDL7	93783	39.09	0.00307	0.00305	7.62
PDL8	93783	39.09	0.00307	0.00312	8.10
PDL9	114659	58.43	0.00307	0.00285	6.84
PDL10-1	94321	39.54	0.02011	0.00215	6.24
PDL10-2	94023	39.29	0.00636	0.00267	7.75
PDL10-3	94321	39.54	0.02011	0.00215	6.24
PDL10-4	94023	39.29	0.00636	0.00267	7.75
PDL11	115139	58.92	0.01179	0.00223	4.60
n	15	15	15	15	15
Mean	98155	43.13	0.0724	0.003	7.17
SD	8366.7	7.77	0.006	0.0003	1.01
COV	0.09	0.18	0.77	0.13	0.14

Notes: E_c = the elastic modulus of concrete; $f'c = \frac{\pi\left(\frac{B}{2}-0.05\right)^2 f'c + \pi\left(\left(\frac{B}{2}\right)^2-\left(\frac{B}{2}-0.05\right)^2\right)}{\pi\left(\frac{B}{2}\right)^2}$; I_c = the moment of inertia of the pile cross-section, (π $b^4/64$); β_r = stiffness ratio between the soil and the pile

Where E_s is the elastic modulus of the surrounding soil. The simplified lateral analysis method by Chang [20] has been adopted in this study. For eccentricity = 0, the pile head displacement and rotation angle are given in Eqs. (3) and (4)

$$\delta = \frac{H}{2EI{\beta_r}^3} \tag{3}$$

$$\alpha(rad) = \frac{H}{2EI{\beta_r}^2} \tag{4}$$

Where H is the lateral load. For eccentricity > 0, the pile head displacement and rotation angle are given in Eqs. (5) and (6)

$$\delta = \frac{(1+e\beta)^3+0.5}{2EI{\beta_r}^3}H \tag{5}$$

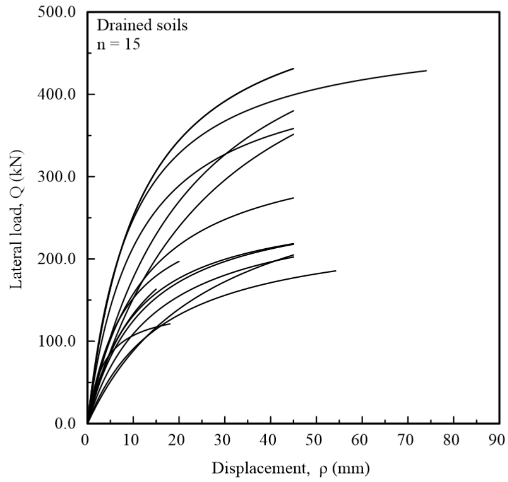

Figure 1. Lateral load versus displacement curves for all piles

$$\alpha(rad) = \frac{(1 + e\beta)^2}{2EI{\beta_r}^2} H \tag{6}$$

3. Lateral interpretation criteria

Interpretation criteria for lateral load tests can be broadly classified into three main categories: lateral displacement, percentage displacement of the pile diameter, and the pile head rotation angle. Additionally, graphical construction methods and mathematical models are employed. The chosen interpretation criteria were selected because they represent different ranges in the distribution of interpreted results. Since most load–displacement curves did not reach 10%B or a pile-head rotation of 5°, each lateral load–displacement dataset was extrapolated to a displacement corresponding to 10% of the pile diameter. According to ASTM D3966, a lateral displacement of 5%B may be adopted as the criterion for determining the ultimate lateral capacity of a drilled shaft. However, considering that pre-bored PC piles generally have smaller diameters, this study adopts 10%B as the upper displacement limit to ensure reasonable analytical interpretation.

Displacement limitation methods define failure based on a specified head displacement. McNulty [23] interprets capacity as the load at 6.4 mm displacement ($Q_{6.4mm}$), Walker and Cox [24] use 12.7 mm ($Q_{12.7mm}$), and the New York City [25] criterion adopts 25.4 mm ($Q_{25.4mm}$). Other methods express displacement as a percentage of the pile diameter. Pyke [26] defines failure at 5% of the diameter ($Q_{5\%B}$), Briaud [27] at 10% ($Q_{10\%B}$), and Broms [3] at 20% ($Q_{20\%B}$).

Rotation limitation methods instead use head slope as the defining measure. Davidson et al. [4] propose a capacity corresponding to a head rotation of 2° ($Q_{2°}$), while Ivey and Dunlap [28] adopt 5° ($Q_{5°}$). Mathematical models have also been introduced. Manoliu et al. [29] define failure as the load corresponding to the inverse slope (1/m) of the line y/p = ms + c, where p is the load and y is the head displacement (Q_H). This method represents an upper bound for all criteria and is called hyperbolic capacity.

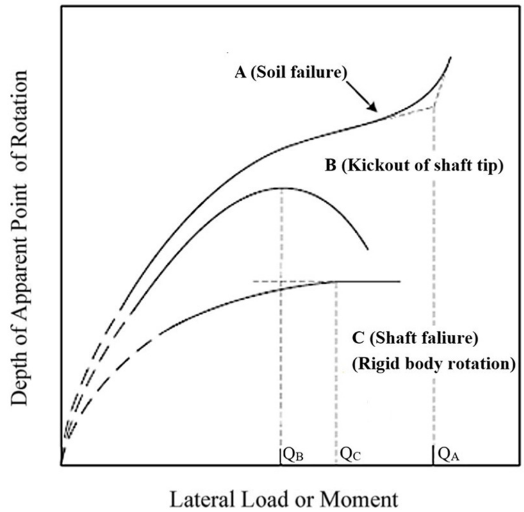

Figure 2. Typical variation of apparent depth of rotation with load [31]

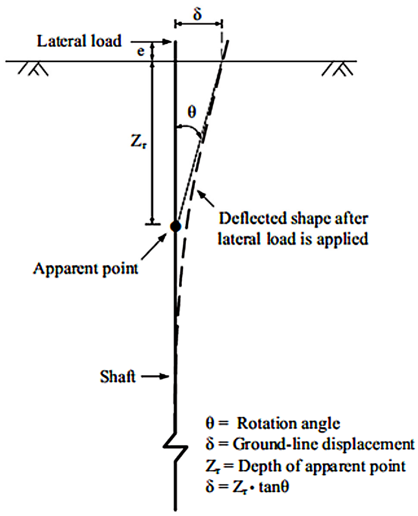

Figure 3. The depth of apparent point of rotation

Finally, graphical construction methods rely on the interpretation of load-displacement curves. Slack and Walker [30] identify capacity from the intersection of two approximate straight lines on a log–log load–displacement plot ($Q_{S\&W}$). Hirany and Kulhawy [31] interpret failure by plotting rotation depth against lateral load and classifying the curves into soil failure (Q_A), pile–soil failure at the pile shaft or pile tip (Q_B), and pile structural failure (Q_C), as illustrated in Fig. 2. The corresponding interpreted failure load is denoted as Q_L. For the lateral limit, the apparent depth of rotation (Z_r) is obtained from the relationship between the lateral displacement (δ) and pile-head rotation (θ), defined as $Z_r = \delta/\theta$, as shown in Fig. 3.

Table 3. References of pre-bored PC pile lateral load tests

Pile No.	Reference
PDL1	Taian Engineering & Technical Consultants Co., Ltd., 2010. Construction of the Yilan City primary power distribution substation turnkey project: Pile test plan.
PDL2	Yantong Engineering Co., Ltd., 2010. Construction of new wind turbine units at Changhua Wangong: Pile load test report.
PDL3	Yantong Engineering Co., Ltd., 2019. Construction of new wind turbine units at Zhanggong (III) and Yongxing wind farms: Pile test report for the Zhanggong (III) site.
PDL4	Taian Engineering & Technical Consultants Co., Ltd., 2006. Construction of the new SM plant at Formosa Chemicals & Fibre Corporation, Mailiao: Static load test report for pre-bored PC piles.
PDL5	Taian Engineering & Technical Consultants Co., Ltd., 2007. Nanya Plastics MGN plant OSBL foundation pile project: Static load test report for foundation piles.
PDL6-1	Taian Engineering & Technical Consultants Co., Ltd., 2006. Mailiao Taiwan Chemical Fiber PC plant phase III expansion project: Static load test report for pre-bored PC piles.
PDL6-2	Taian Engineering & Technical Consultants Co., Ltd., 2006. Mailiao Taiwan Chemical Fiber PC plant phase III expansion project: Static load test report for pre-bored PC piles.
PDL7	Taian Engineering & Technical Consultants Co., Ltd., 2007. Xinguang ABS plant wastewater equalization tank expansion project: Static load test report for pre-bored PC piles.
PDL8	Taian Engineering & Technical Consultants Co., Ltd., 2001. Construction of Anping Port berths 22 and 23 and berth 23 backline project, Tainan: Static load test report for pre-bored PC piles.
PDL9	Cheng Quan Construction Co., Ltd., 2021. Chimei 2×30 MW GTG cogeneration plant project: Pile load test report for pre-bored PC piles.
PDL10-1	Taian Engineering & Technical Consultants Co., Ltd., 2003. Chimei Nankang LCD plant phase IV preliminary pile testing project – Area A: Static load test report for pre-bored PC piles.
PDL10-2	Taian Engineering & Technical Consultants Co., Ltd., 2003. Chimei Nankang LCD plant phase IV preliminary pile testing project – Area A: Static load test report for pre-bored PC piles.
PDL10-3	Taian Engineering & Technical Consultants Co., Ltd., 2003. Chimei Nankang LCD plant phase IV preliminary pile testing project – Area B: Static load test report for pre-bored PC piles.
PDL10-4	Taian Engineering & Technical Consultants Co., Ltd., 2003. Chimei Nankang LCD plant phase IV preliminary pile testing project – Area B: Static load test report for pre-bored PC piles.
PDL11	Cheng He Construction Co., Ltd., 2009. Guiyang primary power distribution substation civil engineering detailed design and construction second turnkey project: Pile test plan

4. Comparison of different interpretation criteria

Table 4 presents the interpreted results of the representative interpretation criteria. Interpreted failure loads were obtained from each load-displacement curve in the database using the interpretation criteria. The range of these capacities is quite wide. For some load tests that were terminated before reaching failure or the interpreted values, the results are reported as greater than 10%B. To facilitate a comprehensive comparison of each method, all interpreted values were normalized by Q_H, which consistently represented the largest value. The results are presented in Table 5, with mean, SD, and COV values. Values in parentheses indicate results within 10%B.

The results show that the mean interpreted Q/Q_H ranges from 0.20 to 0.80 for both the displacement- and rotation-based methods, with the mean values increasing as the movement increases. For the graphical methods, the ratios are $Q_{S\&W}/Q_H$ = 0.42 and Q_L/Q_H = 0.59. The SD values for these methods are generally comparable to those obtained from the other interpretation criteria. In contrast, the COV values fall within the range observed between smaller and larger movements. Notably, this Q_L/Q_H ratio is slightly lower than the Q_L/Q_H = 0.70 reported in the study of drained lateral behavior of drilled shafts by Agaiby et al. [32] and is nearly identical to the 0.60 value in the study of flexible drilled shafts by Chen and Lee [6].

Table 4. Statistical results of various interpretation criteria for pre-bored PC piles in drained soils

Pile No.	Interpreted Capacity, Q (kN)										
	Q_{5mm}	$Q_{6.4mm}$	Q_{8mm}	Q_{10mm}	$Q_{12.7mm}$	Q_{15mm}	Q_{20mm}	$Q_{25.4mm}$	Q_{30mm}	Q_{40mm}	Q_{50mm}
PDL1	57	67	73	86	106	116	130	142	151	168	182
PDL2	103	120	146	164	168	171	196	209	219	230	239
PDL3	86	94	102	107	114	117	123	127	130	133	135
PDL4	85	100	113	130	147	163	187	200	211	228	239
PDL5	165	191	214	242	275	296	327	351	367	391	407
PDL6-1	86	99	110	122	138	151	173	195	200	213	223
PDL6-2	38	49	59	75	97	118	147	155	169	196	213
PDL7	83	100	109	125	141	154	172	185	197	212	223
PDL8	74	85	94	105	117	127	145	161	171	192	211
PDL9	88	104	128	157	180	199	235	271	296	336	365
PDL10-1	144	165	183	201	218	232	253	270	284	310	334
PDL10-2	103	125	139	158	176	188	210	232	247	267	280
PDL10-3	244	275	295	323	360	388	441	477	505	554	590
PDL10-4	110	135	157	190	223	237	276	306	320	365	393
PDL11	168	194	214	235	265	286	335	388	392	421	440
n	15	15	15	15	15	15	15	15	15	15	15
Mean	109	127	142	161	182	196	223	245	257	281	298
SD	50	56	60	65	72	76	87	97	100	110	117
COV	0.46	0.44	0.42	0.40	0.39	0.39	0.39	0.39	0.39	0.39	0.39

Pile No.	Interpreted Capacity, Q (kN)														
	$Q_{0.5\%B}$	$Q_{1\%B}$	$Q_{2\%B}$	$Q_{3\%B}$	$Q_{5\%B}$	$Q_{10\%B}$	$Q_{0.1°}$	$Q_{0.2°}$	$Q_{0.3°}$	$Q_{0.4°}$	$Q_{0.5°}$	$Q_{0.6°}$	$Q_{S\&W}$	Q_L	Q_H
PDL1	47	66	102	127	152	192	67	135	>192	>192	>192	>192	123	179	242
PDL2	74	113	167	192	219	245	74	147	220	>245	>245	>245	160	163	279
PDL3	66	91	112	121	130	137	55	111	>137	>137	>137	>137	74	80	145
PDL4	56	83	128	163	199	239	45	90	136	181	226	>239	118	172	299
PDL5	116	188	270	317	368	418	71	143	214	286	357	>418	177	289	483
PDL6-1	58	86	125	153	192	223	40	81	121	161	202	>223	98	157	270
PDL6-2	20	40	76	127	156	213	40	81	121	161	202	>213	146	171	329
PDL7	50	83	122	153	185	222	46	91	137	182	>222	>222	123	156	277
PDL8	46	72	105	127	160	210	49	98	147	196	>210	>210	123	188	268
PDL9	55	90	157	201	268	365	38	76	114	152	191	229	118	169	562
PDL10-1	140	187	238	268	312	404	151	301	>404	>404	>404	>404	245	-	444
PDL10-2	69	121	173	203	249	289	67	134	200	267	>289	>289	123	177	347
PDL10-3	230	296	400	470	554	679	153	306	459	612	>679	>679	441	604	755
PDL10-4	68	130	216	263	320	414	65	130	194	259	324	388	208	296	564
PDL11	139	201	276	348	408	465	121	243	364	>465	>465	>465	196	361	541
n	15	15	15	15	15	15	15	15	15(12)	15(10)	15(6)	15(2)	14	15	15
Mean	82	123	178	216	240	258	72	144	211(202)	260(246)	290(250)	304(309)	72	144	387
SD	51	65	85	97	106	113	37	74	106(98)	130(142)	130(61)	137(80)	37	74	159
COV	0.63	0.53	0.48	0.45	0.44	0.44	0.52	0.51	0.50(0.51)	0.50(0.53)	0.50(0.26)	0.45(0.26)	0.52	0.51	0.41

The corresponding displacements, denoted as ρ, are listed in Table 6. The values determined from both the displacement and pile diameter percentage limit methods were obtained directly from in-situ measurements. For $Q_{S\&W}$, the corresponding values were approximately 11 mm or 2% of the pile diameter, while for Q_L, they were about 22 mm or 3.5% of the pile diameter. The Q_L method is appropriate for evaluating lateral flexible pre-bored PC piles, as it provides a reasonable

Table 5. Statistical results of normalized interpretation capacities by Manoliu et al. interpretation (Q/Q_H) for drained soils

Pile No.	Normalized Interpreted Capacity, (Q/Q_H)										
	Q_{5mm}	$Q_{6.4mm}$	Q_{8mm}	Q_{10mm}	$Q_{12.7mm}$	Q_{15mm}	Q_{20mm}	$Q_{25.4mm}$	Q_{30mm}	Q_{40mm}	Q_{50mm}
PDL1	0.24	0.28	0.3	0.36	0.44	0.48	0.54	0.59	0.62	0.69	0.75
PDL2	0.37	0.43	0.52	0.59	0.6	0.61	0.7	0.75	0.78	0.82	0.86
PDL3	0.59	0.65	0.7	0.74	0.79	0.81	0.85	0.88	0.9	0.92	0.93
PDL4	0.28	0.33	0.38	0.43	0.49	0.55	0.63	0.67	0.71	0.76	0.8
PDL5	0.34	0.4	0.44	0.5	0.57	0.61	0.68	0.73	0.76	0.81	0.84
PDL6-1	0.32	0.37	0.41	0.45	0.51	0.56	0.64	0.72	0.74	0.79	0.83
PDL6-2	0.12	0.15	0.18	0.23	0.29	0.36	0.45	0.47	0.51	0.6	0.65
PDL7	0.3	0.36	0.39	0.45	0.51	0.56	0.62	0.67	0.71	0.77	0.81
PDL8	0.28	0.32	0.35	0.39	0.44	0.47	0.54	0.6	0.64	0.72	0.79
PDL9	0.16	0.19	0.23	0.28	0.32	0.35	0.42	0.48	0.53	0.6	0.65
PDL10-1	0.32	0.37	0.41	0.45	0.49	0.52	0.57	0.61	0.64	0.7	0.75
PDL10-2	0.3	0.36	0.4	0.46	0.51	0.54	0.61	0.67	0.71	0.77	0.81
PDL10-3	0.32	0.36	0.39	0.43	0.48	0.51	0.58	0.63	0.67	0.73	0.78
PDL10-4	0.2	0.24	0.28	0.34	0.4	0.42	0.49	0.54	0.57	0.65	0.7
PDL11	0.31	0.36	0.4	0.43	0.49	0.53	0.62	0.72	0.72	0.78	0.81
n	15	15	15	15	15	15	15	15	15	15	15
Mean	0.30	0.34	0.39	0.44	0.49	0.53	0.6	0.65	0.68	0.74	0.78
SD	0.11	0.11	0.12	0.12	0.12	0.11	0.11	0.11	0.10	0.09	0.08
COV	0.36	0.34	0.32	0.28	0.24	0.21	0.18	0.16	0.15	0.12	0.10

Pile No.	Normalized Interpreted Capacity, (Q/Q_H)													
	$Q_{0.5\%B}$	$Q_{1\%B}$	$Q_{2\%B}$	$Q_{3\%B}$	$Q_{5\%B}$	$Q_{10\%B}$	$Q_{0.1°}$	$Q_{0.2°}$	$Q_{0.3°}$	$Q_{0.4°}$	$Q_{0.5°}$	$Q_{0.6°}$	$Q_{S\&W}$	Q_L
PDL1	0.19	0.27	0.42	0.52	0.57	0.63	0.28	0.56	>0.79	>0.79	>0.79	>0.79	0.51	0.74
PDL2	0.27	0.41	0.60	0.69	0.74	0.78	0.27	0.53	0.79	>0.88	>0.88	>0.88	0.57	0.58
PDL3	0.46	0.63	0.77	0.83	0.87	0.90	0.38	0.77	>0.94	>0.94	>0.94	>0.94	0.51	0.55
PDL4	0.19	0.28	0.43	0.55	0.63	0.67	0.15	0.30	0.45	0.61	0.76	>0.80	0.39	0.58
PDL5	0.24	0.39	0.56	0.66	0.72	0.76	0.15	0.30	0.44	0.59	0.74	>0.87	0.37	0.60
PDL6-1	0.21	0.32	0.46	0.57	0.66	0.71	0.15	0.30	0.45	0.60	0.75	>0.83	0.36	0.58
PDL6-2	0.06	0.12	0.23	0.39	0.45	0.47	0.12	0.25	0.37	0.49	0.61	>0.65	0.44	0.52
PDL7	0.18	0.30	0.44	0.55	0.61	0.67	0.17	0.33	0.49	0.66	>0.80	>0.80	0.44	0.56
PDL8	0.17	0.27	0.39	0.47	0.54	0.60	0.18	0.37	0.55	0.73	>0.78	>0.78	0.46	0.70
PDL9	0.10	0.16	0.28	0.36	0.42	0.48	0.07	0.14	0.20	0.27	0.34	0.41	0.21	0.30
PDL10-1	0.32	0.42	0.54	0.60	0.65	0.70	0.34	0.68	>0.91	>0.91	>0.91	>0.91	0.55	-
PDL10-2	0.20	0.35	0.50	0.59	0.66	0.72	0.19	0.39	0.58	0.77	>0.83	>0.83	0.35	0.51
PDL10-3	0.30	0.39	0.53	0.62	0.69	0.73	0.20	0.41	0.61	0.81	>0.90	>0.90	0.58	0.80
PDL10-4	0.12	0.23	0.38	0.47	0.53	0.57	0.12	0.23	0.34	0.46	0.57	0.69	0.37	0.52
PDL11	0.26	0.37	0.51	0.64	0.71	0.75	0.22	0.45	0.67	>0.86	>0.86	>0.86	0.36	0.67
n	15	15	15	15	15	15	15	15	15(12)	15(10)	15(6)	15(2)	15	14
Mean	0.22	0.33	0.47	0.57	0.63	0.68	0.20	0.40	0.57(0.50)	0.69(0.60)	0.76(0.63)	0.80(0.55)	0.42	0.59
SD	0.09	0.12	0.13	0.12	0.11	0.11	0.08	0.17	0.21(0.15)	0.18(0.15)	0.15(0.15)	0.13(0.14)	0.10	0.12
COV	0.43	0.35	0.27	0.20	0.18	0.16	0.42	0.42	0.36(0.30)	0.27(0.26)	0.20(0.23)	0.16(0.26)	0.23	0.20

interpretation of both capacity and displacement. For practical and convenient application, the load corresponding to either 20 mm displacement or 3%B is the closest to Q_L. The mean normalized Q/Q_H versus mean displacement and displacement based on percentage diameter curves are shown in Figs. 4(a) and 4(b), respectively.

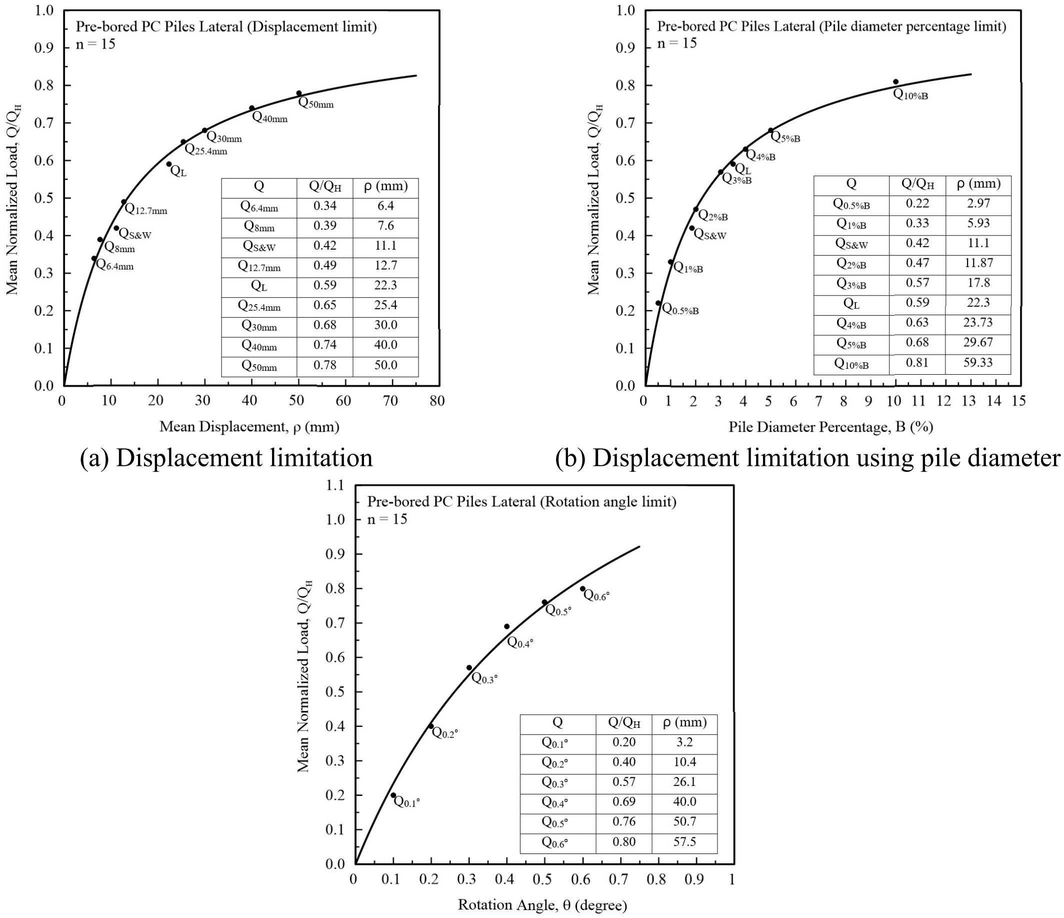

(a) Displacement limitation (b) Displacement limitation using pile diameter

(c) Pile head rotation limitation

Figure 4. Results of the mean normalized load-displacement curve

Due to insufficient load test data of pile-head rotation, this study adopted the simplified lateral analysis method proposed by Chang [20] to estimate the pile-head rotation. This method, which assumes linear behavior, is commonly applied in field lateral analysis. As observed from Fig. 4(c), the interpreted results exhibit linear behavior in the initial portion of the curve, whereas the extended portion of the curve gradually levels off. Therefore, the use of Chang's method should be exercised with caution due to its linear assumption.

A regression analysis was performed comparing three methods, $Q_{10\%B}$, $Q_{S\&W}$, and Q_L, against a reference capacity Q_H, with the results detailed in Table 7 and visualized in Fig. 5. The analysis revealed that all three methods underestimate the reference capacity, as evidenced by all regression slopes being less than 1.0. Among the methods, $Q_{10\%B}$ proved to be the most reliable and consistent predictor, showing an exceptionally high coefficient of determination (r^2 = 0.92) and the closest slope to unity, indicating a strong linear correlation with Q_H. Conversely, $Q_{S\&W}$ was determined to exhibit the lowest correlation (r^2 = 0.65) and the most severe underestimation of the capacity, which corresponds visually to the greatest scatter and the lowest regression line in the figure. The Q_L method was intermediate, with r^2 = 0.74

Table 6. Statistical results of interpreted displacement for pre-bored PC piles in drained soils

Pile No.	Interpreted displacement, ρ (mm)														
	$\rho_{0.5\%B}$	$\rho_{1\%B}$	$\rho_{2\%B}$	$\rho_{3\%B}$	$\rho_{4\%B}$	$\rho_{5\%B}$	$\rho_{10\%B}$	$\rho_{0.1°}$	$\rho_{0.2°}$	$\rho_{0.3°}$	$\rho_{0.4°}$	$\rho_{0.5°}$	ρ_{L}	$\rho_{S\&W}$	ρ_{H}
PDL1	3	6	12	18	24	30	60	6.2	21.7	>60	>60	>60	46.6	16.5	>60
PDL2	3	6	12	18	24	30	60	3.7	8	32.5	>60	>60	11.5	8.6	>60
PDL3	3	6	12	18	24	30	60	2.2	11.3	>60	>60	>60	4.4	3.7	>60
PDL4	2.5	5	10	15	20	25	50	2.2	5.7	11.5	19	39.2	16.9	8.5	>50
PDL5	3	6	12	18	24	30	60	1.7	4.3	8.1	14.2	26.9	14.2	5.6	>60
PDL6-1	2.5	5	10	15	20	25	50	2	4.6	9.4	16.8	32	15.7	6.1	>50
PDL6-2	2.5	5	10	15	20	25	50	5.5	10.5	15.2	28	43.7	30	19.8	>50
PDL7	2.5	5	10	15	20	25	50	2.5	5.8	12.3	24	>50	15.3	8.5	>50
PDL8	2.5	5	10	15	20	25	50	2.7	8.6	20.2	43	>50	37.9	20.2	>50
PDL9	2.5	5	10	15	20	25	50	2.5	4.6	8	11.1	16.8	7.6	7.3	>50
PDL10-1	4	8	16	24	32	40	80	5.3	36.4	>80	>80	>80	-	17.5	>80
PDL10-2	3	6	12	18	24	30	60	3	7.4	17.5	40.1	>60	13.4	6.4	>60
PDL10-3	4	8	16	24	32	40	80	2	9	23.3	56	>80	53.5	20	>80
PDL10-4	3	6	12	18	24	30	60	3	6.2	10.5	18	32	22.9	11.5	>60
PDL11	3.5	7	14	21	28	35	70	3	11.3	23	>70	>70	22.4	6.6	>70
n	15	15	15	15	15	15	15	15	15	15 (12)	15 (10)	15(6)	15 (14)	15	15
Mean	2.97	5.93	11.87	17.80	23.73	29.67	59.33	3.17	10.36	26.10	40.01	50.71	22.31	11.12	59.33
SD	0.50	1.00	2.00	2.99	3.99	4.99	9.98	1.35	8.13	21.71	22.10	18.32	14.11	5.74	9.98
COV	0.17	0.17	0.17	0.17	0.17	0.17	0.17	0.43	0.78	0.83	0.55	0.36	0.63	0.52	0.17

5. Comparison of interpretation criteria for different pile types

Based on the three categories of interpretation criteria for lateral capacity, a comparison among different pile types was conducted. The lateral behavior of Pre-bored PC piles was compared with that of flexible drilled shafts [6], rigid drilled shafts [33], drilled shafts in gravel layers [34], and flexible driven piles [35]. The normalized interpreted failure loads for different pile types are presented in Fig. 6. The corresponding normalized curves are represented by Curve A for pre-bored PC piles, Curve B for flexible drilled shafts, Curve C for rigid drilled shafts, Curve D for drilled shafts in gravel layers, and Curve E for flexible driven piles. Detailed data and references are listed in Table 8. When capacities are normalized by Q_H, as shown in Figs. 6(a) and 6(b), the behavior of the curves of different pile types converges and becomes less distinct. This trend aligns with observations by Topacio et al. [36] regarding drilled shafts in rock; while raw load-displacement curves vary significantly between soft and hard rock due to stiffness, the distinction between the two diminished substantially after normalizing the load. After normalization, pre-bored PC piles show curve stiffness comparable to driven piles and drilled shafts in gravel. Overall, pre-bored PC piles exhibited higher normalized lateral capacities than drilled shafts and driven piles.

For pile-head rotation angle, all three pile types exhibited a linear trend, as shown in Fig. 6(c). This behavior is likely influenced by the common use of the simplified lateral analysis method by

Table 7. Regression data comparison for different methods versus Q_H

Interpretation, Q (kN)	X	Statistics			
		n	r^2	SD (kN)	R
$Q_{10\%B}$	0.82	15	0.92	137	542
$Q_{S\&W}$	0.43	15	0.65	74	367
Q_L	0.6	14	0.74	37	524

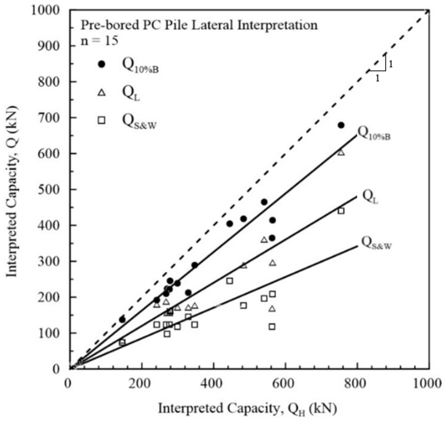

Figure 5. Comparison of the regression results of the lateral interpretation criteria

Table 8. Comparison of normalized interpreted failure loads for different pile types

Pile types (drained data)	Reference	Mean normalized interpreted load, (Q/Q_H)											
		Q_{5mm}	$Q_{6.4mm}$	Q_{8mm}	Q_{10mm}	$Q_{12.7mm}$	Q_{15mm}	Q_{20mm}	$Q_{25.4mm}$	Q_{30mm}	Q_{40mm}	Q_{50mm}	$Q_{0.5\%B}$
Pre-bored PC piles (n =15)	This study	0.30	0.34	0.39	0.44	0.49	0.53	0.6	0.65	0.68	0.74	0.78	0.22
Flexible drilled shafts (n = 56)	Chen and Lee [6]	0.33	-[a]	0.41	0.44	0.48	0.51	0.56	0.59	0.62	0.65	0.67	0.28
Rigid drilled shafts (n = 20)	Chen et al. [33]	0.32	-[a]	-[a]	-[a]	0.39	-[a]	-[a]	0.49	-[a]	-[a]	0.64	0.34
Drilled shafts in gravel (n = 24)	Marcos and Chen [34]	0.35	-[a]	-[a]	0.48	-[a]	0.57	0.62	0.66	0.70	-[a]	-[a]	0.36
Flexible driven piles (n = 19)	Wu [35]	0.29	0.33	0.39	0.44	0.49	0.52	0.59	0.64	0.67	0.73	0.77	0.18
	Mean	0.32	0.34	0.40	0.45	0.46	0.53	0.59	0.61	0.67	0.71	0.72	0.28
	SD	0.02	0.01	0.01	0.02	0.04	0.02	0.02	0.06	0.03	0.04	0.06	0.07
	COV	0.07	0.01	0.02	0.04	0.09	0.04	0.04	0.10	0.04	0.06	0.09	0.25

Pile types (drained data)	Reference	Mean normalized interpreted load, (Q/Q_H)										
		$Q_{1\%B}$	$Q_{2\%B}$	$Q_{3\%B}$	$Q_{5\%B}$	$Q_{10\%B}$	$Q_{0.1°}$	$Q_{0.2°}$	$Q_{0.3°}$	$Q_{0.4°}$	$Q_{0.5°}$	$Q_{0.6°}$
Pre-bored PC piles (n =15)	This study	0.33	0.47	0.57	0.68	0.81	0.20	0.40	>0.57[b]	>0.69[b]	>0.76[b]	>0.80[b]
Flexible drilled shafts (n = 56)	Chen and Lee [6]	0.38	0.50	0.57	0.64	0.70	0.15	0.30	>0.43[b]	>0.52[b]	>0.59[b]	>0.64[b]
Rigid drilled shafts (n = 20)	Chen et al. [33]	-[a]	0.48	-[a]	0.64	0.76	-[a]	0.29	-[a]	0.36	-[a]	0.46
Drilled shafts in gravel (n = 24)	Marcos and Chen [34]	0.48	0.61	0.68	0.74	-[a]	0.42	0.56	0.62	0.73	-[a]	-[a]
Flexible driven piles (n = 19)	Wu [35]	0.30	0.44	0.52	0.63	0.76	0.10	0.20	0.30	0.41	0.52	0.62
	Mean	0.37	0.50	0.59	0.67	0.76	0.22	0.35	>0.48[b]	>0.54[b]	>0.62[b]	>0.63[b]
	SD	0.07	0.06	0.06	0.04	0.04	0.12	0.12	0.13	0.15	0.10	0.12
	COV	0.18	0.12	0.10	0.06	0.05	0.56	0.35	0.26	0.27	0.16	0.19

Note: [a]No data, [b]beyond extrapolated curve

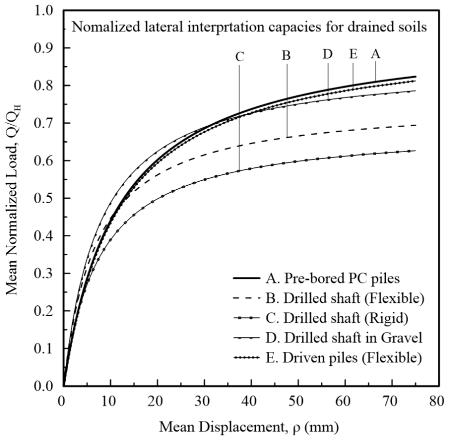

(a) Displacement limitation

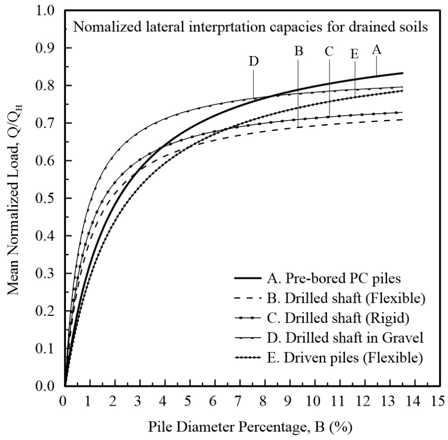

(b) Percentage limitation using pile diameter

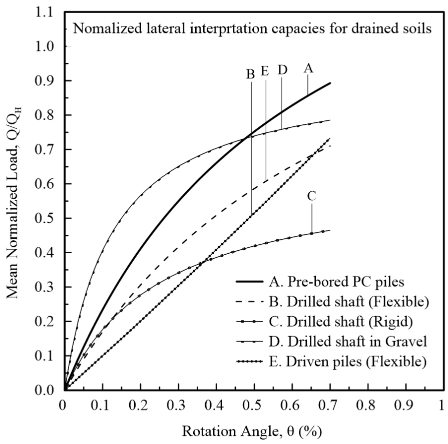

(c) Rotation angle

Figure 6. Comparison of mean normalized curves of different pile types

Chang [20] in Eqs. (3)-(6). Before reaching a pile-head rotation of 5°, drilled shafts in gravel layers show higher normalized interpreted loads than all other pile types. As rotation continues to increase, the curve gradually flattens, indicating that the behavior approaches the ultimate state. At the same rotation angle, pre-bored PC piles sustained higher normalized interpreted loads. Although pre-bored PC piles are classified as flexible foundations with smaller diameters, the higher concrete strength enabled them to mobilize larger loads at greater pile-head rotation angles.

6. Conclusions

Lateral load test data for flexible pre-bored PC piles in drained soils were analyzed using representative interpretation criteria. A comprehensive evaluation was conducted, from which conclusions were drawn.

1. Q_H gives the highest values and always lies above the measurement, while loads at 30 mm, 10%B, and 0.4° are comparable with the mean capacities close to $0.7Q_H$.

2. The mean ratio of $Q_{S\&W}$ is $0.42Q_H$ and occurs at approximately occurs at 11 mm and 2%B. Meanwhile, Q_L is approximately $0.59Q_H$ and is about 22 mm and 3%B.
3. The Q_L method is appropriate for evaluating lateral flexible pre-bored PC piles, as it provides a reasonable interpretation of both capacity and displacement. For practical and convenient applications, the load corresponding to either 20 mm displacement or 3% of the pile diameter (B) is the closest to Q_L and can be considered as Q_L.
4. The estimation of pile-head rotation using Chang's method provides a practical and simplified approach. However, its assumption of linear behavior necessitates cautious application.
5. Regression analysis showed that $Q_{10\%B}$ proved to be the most reliable and consistent predictor, showing a high coefficient of determination (r^2 = 0.92) and the closest slope to unity, indicating a strong linear correlation with Q_H.
6. After normalization by Q_H, the responses of different pile types become more comparable. Pre-bored PC piles show curve stiffness comparable with driven piles and drilled shafts in gravel. Overall, pre-bored PC piles exhibited higher normalized lateral capacities than drilled shafts and driven piles.

Acknowledgments

This study was supported by the Taiwan National Science and Technology Council under contract No. NSTC 112-2221-E-033-022-MY3 and John Su Foundation under contract No. CYCU 1120623.

References

1. Pérez, J.A., Ponce-Torres, A., Ríos, J.D., Sánchez-González, E. (2024). Fatigue behavior of H-section piles under lateral loads in cohesive soil. Buildings, 14(10), 3228. https://doi.org/10.3390/buildings14103228.
2. Wu, J.J., Pu, L.J., Zhai, C.M. (2024). A review of static and dynamic p-y curve models for pile foundations. Buildings, 14(6), 1507. https://doi.org/10.3390/buildings14061507.
3. Broms, B.B. (1964). Lateral resistance of piles in cohesionless soils. Journal of the Soil Mechanics and Foundations Division, 90(3), 123-156. https://doi.org/10.1061/JSFEAQ.0000614.
4. Davidson, H.L., Cass, P.G., Khilji, K.H., McQuade, P.V. (1982). Laterally loaded drilled pier research. Report No. EL-2197; Electric Power Research Institute, Palo Alto, California.
5. Carter, J.P., Kulhawy, F.H. (1992). Analysis of laterally loaded shafts in rock. Journal of Geotechnical Engineering, 118(6), 839-855. https://doi.org/10.1061/(ASCE)0733-9410(1992)118:6(839).
6. Chen, Y.J., Lee, Y. (2010). Evaluation of lateral interpretation criteria for drilled shaft capacity. Journal of Geotechnical and Geoenvironmental Engineering, 136(8), 1124-1136. https://doi.org/10.1061/(ASCE)GT.1943-5606.0000325.
7. Poorjafar, A., Esmaeili-Falak, M., Katebi, H. (2021). Pile-soil interaction determined by laterally loaded fixed head pile group. Geomechanics and Engineering, 26(1), 13-25. https://doi.org/10.12989/gae.2021.26.1.013.
8. Wang, H., Wang, L.Z., Askarinejad, A., Hong, Y., He, B. (2023). Ultimate soil resistance of the laterally loaded pile in uniform sand. Canadian Geotechnical Journal, 60(4), 587-593. https://doi.org/10.1139/cgj-2021-0487.
9. Phanikanth, V.S., Choudhury, D., Srinivas, K. (2013). Response of flexible piles under lateral loads. Indian Geotechnical Journal, 43, 76-82. https://doi.org/10.1007/s40098-012-0030-6.

10. Chou, S.A., Chen, Y.J., Chiou, J.S., Topacio, A., Marcos, M.C. (2022). Evaluation of lateral capacity for flexible drilled shafts in cohesionless soils. Science Progress, 105, 1-30. https://doi.org/10.1177/00368504221113195.
11. Hsiao, M.H., Chen, Y.J., Phoon, K.K., Jos, M.A. (2025). Statistical evaluation of pre-bored PC pile behavior under axial compression. Georisk: Assessment and Management of Risk for Engineered Systems and Geohazards, 1-44. https://doi.org/10.1080/17499518.2025.2549417.
12. Chen, Y.J., Jos, M.A., Topacio, A., Wang, K. (2025a). Uplift capacity and displacement of pre-bored PC piles in undrained soils. International Journal of Engineering and Technology Innovation, 15, 300-313. https://doi.org/10.46604/ijeti.2024.14597.
13. Chen, Y.J., Wang, K., Phoon, K.K., Guo, M., Jos, M.A. (2025b). Pre-bored PC pile capacity prediction in drained soils using artificial neural network. ASCE-ASME Journal of Risk and Uncertainty in Engineering Systems, Part A: Civil Engineering, 11, 1-26. https://doi.org/10.1061/AJRUA6/RUENG-1737.
14. Chen Y.J., Liao, M.R., Lin, S.S., Huang J.K., Marcos, M.C. (2014). Development of an integrated web-based system with a pile load test database and pre-analyzed data. Geomechanics and Engineering, 7(1), 37-53. https://doi.org/10.12989/gae.2014.7.1.037
15. Chen, Y.J., Topacio, A., Laveti, S., Jos, M.A., Hsiao, M.H. (2024). Development and use of CYCU pile load test database. Databases for Data-Centric Geotechnics, CRC Press, Taylor & Francis Group, Chapter 4, 163-212.
16. Chen, Y.J., Jos, M.A. (2025). Introduction to CYCU pile load test database. Geodata and AI, 100034. https://doi.org/10.1016/j.geoai.2025.100034.
17. Chen, C.J., Yi, H., Stanley, N. (2025c). Conditional similarity triplets enable covariate-informed representations of single-cell data. BMC Bioinformatics, 26, 45. https://doi.org/10.1186/s12859-025-06069-5
18. Chen, C.J., Chen, Y., Yun, S., Stanley, N., Chen, T. (2025d). Spatial coordinates as a cell language: A multi-sentence framework for imaging mass cytometry analysis. In: Findings of the Association for Computational Linguistics: ACL 2025, 13241-13252, Vienna, Austria.
19. Poulos, H.G., Hull, T.S. (1989). Role of analytical geomechanics in foundation engineering. Foundation Engineering: Current Principles and Practices (GSP 22), (Ed., F.H. Kulhawy); ASCE, New York, 1578-1606.
20. Chang, Y.L. (1937). Lateral pile loading tests. Transactions of the American Society of Civil Engineers, 102, 273-276.
21. Fukuoka, M., Uto, K. (1959). Measurement of the coefficient of subgrade reaction in the horizontal direction using a borehole. Tsuchi-to-Kiso (Soil mechanics and Foundation Engineering), Special Issue No. 1.
22. Ohya, S., Imai, I., Matsubara, M. (1982). Relationships between N value by SPT and LLT pressuremeter results. Proceedings of the 2nd European Symposium on Penetration Testing, Amsterdam.
23. McNulty, J.F. (1956). Thrust loading on piles. Journal of the Soil Mechanics and Foundations Division, 82(2), 1-25. https://doi.org/10.1061/JSFEAQ.0000009.
24. Walker, J.N., Cox, E.H. (1966). Design of pier foundations for lateral loads. Transactions of the ASAE, 9(3), 417-420.
25. New York City (1981). Building code of the city of New York, Gould Publications, Binghamton.
26. Pyke, R. (1984). Panel discussion: laterally loaded deep foundation (STP 835). ASTM; Philadelphia, 239-243.
27. Briaud, J.L. (1984). Panel discussion: laterally loaded deep foundation (STP 835). ASTM; Philadelphia, 239-243.
28. Ivey, D.L., Dunlap, W.A. (1970). Design procedure compared to full-scale tests of drilled shaft footings. Report No. 105-3. University of Texas, Austin, Texas.
29. Manoliu, I., Dimitriu, D.V., Radulescu, N., Dobrescu, G. (1985). Load-deflection characteristics of drilled piers. Proceedings of the 11th Int. Conf. on Soil Mech. Found. Eng., 3, 1553-1558.

30. Slack, D.C., Walker, J.N. (1970). Deflections of shallow pier foundations. Journal of the Soil Mechanics and Foundations Division, 96(4), 1143-1157. https://doi.org/10.1061/JSFEAQ.0001432.
31. Hirany, A., Kulhawy, F.H. (1989). Interpretation of load tests on drilled shafts. 3: lateral and moment. Foundation Engineering: Current Principles and Practices (GSP 22), (Ed., F.H. Kulhawy), ASCE, New York, 1160-1172.
32. Agaiby, S.W., Kulhawy, F.H., Trautmann, C.H. (1992). Experimental study of drained lateral and moment behavior of drilled shafts during static and cyclic loading. Report TR-100223. Electric Power Research Institute, Palo Alto, California.
33. Chen, Y.J., Lin, S.W., Kulhawy, F.H. (2011). Evaluation of lateral interpretation criteria for rigid drilled shafts. Canadian Geotechnical Journal, 48, 634-643. https://doi.org/10.1139/t10-094.
34. Marcos, M.C., Chen, Y.J. (2013). Evaluation of lateral interpretation criteria for drilled shaft capacity in gravels. Geotechnical and Geological Engineering, 31, 1411-1420. https://doi.org/10.1007/s10706-013-9665-z
35. Wu, Y.W. (2014). Evaluation of lateral behavior for driven piles. Master's Thesis, Chung Yuan Christian University, Taiwan
36. Topacio, A., Chen, Y.J., Phoon, K.K., Tang, C. (2024). Evaluation of compression interpretation criteria for drilled shafts socketed into rocks. Proceedings of the Institution of Civil Engineers - Geotechnical Engineering, 177, 17-33. https://doi.org/10.1680/jgeen.21.00120.

Notation list

Symbol	Definition
B	Pile diameter
D_r	Relative density
E_c	Elastic modulus of concrete
E_s	Elastic modulus for soil
e	Height of pile head above ground surface
f'_c	Compressive strength of concrete
GWT	Ground water table
H	Lateral load
I_c	Moment of inertia of the pile cross-section
K_h	Initial modulus of subgrade reaction
L	Pile length
Lc	Critical pile length
n	Number of data points
R	Range
SD	Standard deviation
X	Normalized mean value
Z_r	Depth of apparent point
α	Pile-head rotation angle
β_r	Stiffness ratio between the soil and the pile
γ_t	Total unit weight
δ	Pile head displacement
φ'	Effective friction angle
θ	Pile-head rotation